First International Conference on
Bio-based Building Materials

June 22nd - 24th 2015
Clermont-Ferrand, France

EFFECT OF CALCINED NANOCLAY ON MICROSTRUCTURAL AND MECHANICAL PROPERTIES OF CHEMICALLY TREATED HEMP FABRIC-REINFORCED CEMENT NANOCOMPOSITES

Hakamy A[1, 2], Shaikh FUA[3], Low IM[1]

[1]Department of Imaging & Applied Physics, Curtin University, Perth, Australia
[2]Department of Physics, Umm Al-Qura University, Makkah, Saudi Arabia
[3]Department of Civil Engineering, Curtin University, Perth, Australia

*Corresponding author. Email: j.low@curtin.edu.au

Abstract
Calcined nanoclay was prepared in this paper by heating nanoclay (Cloisite 30B) at 900° C for 2h. This study presents the influence of calcined nanoclay (CNC) and chemical treatment on the microstructure and mechanical properties of treated hemp fabric-reinforced cement nanocomposites. Characterisation of microstructure is investigated using Quantitative X-ray Diffraction Analysis (QXDA) and High Resolution Transmission Electron Microscopy (HRTEM). The optimum hemp fabric content is 6.9 wt% (i.e. 6 fabric layers). Alkali treated hemp fabric-reinforced cement composites exhibited the highest flexural strength and fracture toughness when compared to their non-treated counterparts. In addition, mechanical properties are improved as a result of CNC addition. An optimum replacement of ordinary Portland cement with 1 wt% CNC is observed through reduced porosity and increased density, flexural strength and fracture toughness in treated hemp fabric-reinforced nanocomposite. The microstructural analysis such as QXDA indicates that the CNC behaves not only as a filler to improve the microstructure, but also as the activator to support the pozzolanic reaction and thus improved the adhesion between the treated hemp fabric and the matrix.

Keywords:
Nanoclay, hemp fabrics, cement, mechanical properties, microstructure.

1 INTRODUCTION

Nowadays, nanotechnology is one of the most active research areas in the civil engineering and construction materials [Sancher et al. 2010, Hakamy et al. 2014]. In the construction industry, several types of nanomaterials have been incorporated into concretes such as nano-SiO_2 and nano-ZrO_2 in order to improve the durability and mechanical properties of concrete and Portland cement matrix [Nazari et al. 2011, Jo et al. 2007]. Recently, natural short fibres are gaining increasing popularity to develop 'environmental-friendly construction materials' as alternative to synthetic fibres in fibre-reinforced concrete [Sedan et al. 2008]. In contrast, the use of natural fibre sheets and fabrics is more prevalent in polymer matrix when compared to cement-based matrix [Alamri et al. 2012]. However, one of the major drawbacks of natural fibres is relatively weak fibres–matrix interface which can adversely affect the mechanical properties of natural fibre reinforced cement composites [Pacheco-Torgal et al. 2011, Hakamy et al. 2014]. In this paper, the use of CNC in hemp fibre-reinforced cement composite is expected to overcome the above disadvantage of hemp fibres in cementitious composites.

2 EXPERIMENTAL PROCEDURE

2.1 Materials

The nanoclay platelets (Cloisite 30B) were supplied by Southern Clay Products, USA. The woven hemp fabric with 0.54 mm thickness and 0.3 mm opening size between bundles was supplied by Hemp Wholesale Australia Pty. Kalamunda, Western Australia. Ordinary Portland cement (ASTM Type I) was used in all mixes. Calcined nanoclay (CNC) was prepared by heating the nanoclay at 800, 850 and 900° C for 2 h. It is found in this study that nanoclay transferred to amorphous state (calcined nanoclay) at 900 °C. Moreover many platelets in calcined nanoclay were destroyed and some of them broken to small nanoparticles with average size 5 nm (Fig. 1). In order to treat the surface of the fibres, the hemp fabrics were chemically treated by 1.7 M NaOH solution (pH=14) for 48 hours, details in the reference (Sedan 2008).

2.2 Sample preparation and curing

Nanocomposites

The ordinary Portland cement (OPC) is partially substituted by calcined nanoclay (CNC) of 1, 2 and 3 % by weight of OPC. The OPC and CNC were first dry mixed for 15 minutes in Hobart mixer. The binder is CNC -cement powder. The cement nanocomposite matrix was prepared with a water / binder ratio of 0.485.

Untreated and treated hemp fabric-reinforced cement composites

Firstly, the 4, 5, 6, 7 layers of un-treated hemp fabrics and the 6 layers of treated hemp fabrics were first soaked into the cement matrix and then laid on polished timber mould by hand. After that, the compacted fabrics were left under heavy weight (30 kg) for 1 hour to reduce air bubbles and voids inside the specimens. Secondly, a thin layer of cement matrix was poured into the prismatic mould followed by the compacted pre-soaked hemp fabrics into the mould. Finally a thin layer of matrix was poured into the mould as upper layer and the specimens were left for 24 hours to cure at room temperature. Un-treated hemp fabric-reinforced cement composites are fabricated with different weight percentages of hemp fabrics: 4.5 wt% (4 layers of fabrics), 5.7 wt% (5 layers of fabrics), 6.9 wt% (6 layers of fabrics) and 8.1 wt% (7 layers of fabrics).The content of treated hemp fabrics in composite was about 6.9 wt%.

Treated hemp fabric-reinforced nanocomposites

Only 6 layers of treated hemp fabrics were used to reinforce the nanocomposite matrix. The fabrication steps are similar to that of UHFRC described before. The treated hemp fabric-reinforced nanocomposite containing 1, 2 and 3 wt% calcined nanoclay is termed as 6THFR-CNCC1, 6THFR-CNCC2 and 6THFR-CNCC3, respectively. The total amount of treated hemp fabrics in each nanocomposite was about 6.9 wt%. The mix proportions are given in Table 1. The position through the depth of sample for 6 treated hemp fabric layers is indicated in Fig 2. Five prismatic plate specimens of 300×70×10 mm in dimension were cast for each series and all specimens were demolded after 24 h of casting and kept under water for approximately 56 days. Five rectangular specimens of each series with dimensions 70×20×10 mm were cut from the fully cured prismatic plate for each mechanical and physical test.

2.3 Characterisation

HRTEM imaging was done using 3000F (JEOL company) operating at 300 kV. The Quantitative X-ray Diffraction Analysis (QXDA) with Rietveld refinement was done with Bruker *DIFFRAC*^{plus} TOPAS software associated with the International Centre for Diffraction Data PDF-4 2013 database. Scanning electron microscopy (SEM) imaging was obtained using a NEON 40ESB, ZEISS.

2.4 Apparent Porosity, density, flexural strength and Fracture Toughness Test

The apparent porosity and density were determined according to the ASTM Standard (C-20). Three-point bend tests were conducted using a LLOYD Material Testing Machine to evaluate the flexural strength and fracture toughness of the composites. The support span used was 40 mm with a displacement rate of 0.5 mm/min. The ratio of crack length to depth was about 1/3 [Hakamy et al. 2014].

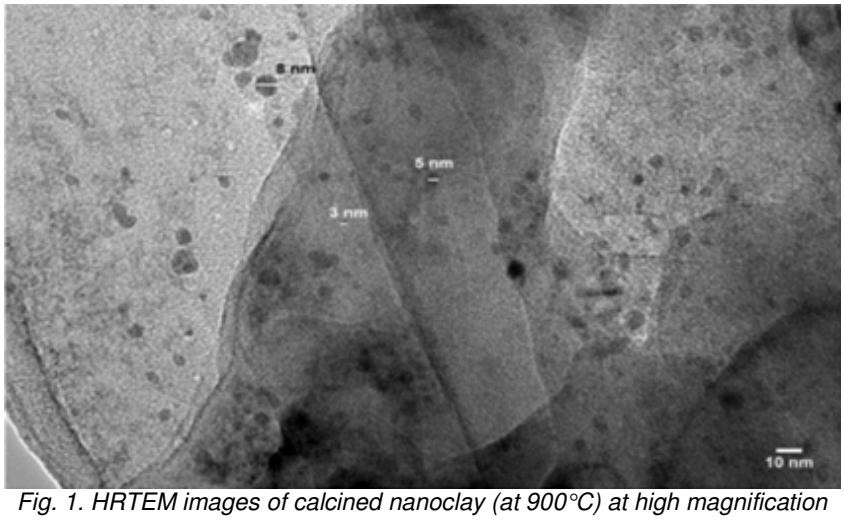

Fig. 1. HRTEM images of calcined nanoclay (at 900°C) at high magnification

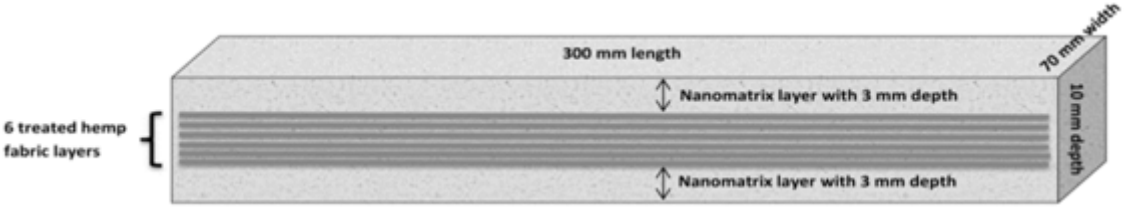

Fig.2. Schematic representation of 6 treated hemp fabric layers position through the depth of cement nanocomposite matrix

Tab. 1: Mix proportions of specimens

Sample	Hemp fabric (HF)		Mix proportions (wt %)		
	Content (wt %)	Fabric layers	Cement	CNC	Water/binder
C	0	0	100	0	0.485
4UHFRC	4.5	4	100	0	0.485
5UHFRC	5.7	5	100	0	0.485
6UHFRC	6.9	6	100	0	0.485
7UHFRC	8.1	7	100	0	0.485
6THFRC	6.9	6	100	0	0.485
CNCC1	0	0	99	1	0.485
CNCC2	0	0	98	2	0.485
CNCC3	0	0	97	3	0.485
6THFR-CNCC1	6.9	6	99	1	0.485
6THFR-CNCC2	6.9	6	98	2	0.485
6THFR-CNCC3	6.9	6	97	3	0.485

Tab. 2: QXDA results for cement paste and nanocomposites containing 1, 2 and 3 wt% CNC

	Weight % (Phase abundance)			
Phase	C	CNCC1	CNCC2	CNCC3
Portlandite [$Ca(OH)_2$]	16.8	12.1	13.2	14.1
Ettringite [$Ca_6Al_2(SO_4)_3(OH)_{12}.26H_2O$]	2.0	1.3	1.5	1.8
Tricalcium silicate [C_3S]	1.3	2.0	1.7	1.4
Dicalcium silicate [C_2S]	4.4	6.6	6.1	5.4
Gypsum [$Ca(SO_4)(H_2O)_2$]	0.7	0.4	0.6	0.4
Calcite [$CaCO_3$]	3.7	2.1	2.7	3.3
Quartz [SiO_2]	0.9	0.6	0.4	0.7
Amorphous content	70.1	74.8	73.7	72.8

Tab. 3: Porosity (P_S), density (ρ), flexural strength (σ_F) and Fracture toughness (K_{IC}) values for cement paste, untreated hemp fabric-reinforced cement composite (UHFRC), 6THFRC composites, nanocomposites and 6THFR-CNCC nanocomposites.

Sample	P_S (%)	ρ (g/cm^3)	σ_F (MPa)	K_{IC} (MPa.m$^{1/2}$)
C	23.93	1.76	5.42	0.35
4UHFRC	30.14	1.61	10.21	1.07
5UHFRC	31.58	1.56	11.26	1.26
6UHFRC	33.02	1.53	12.64	1.41
7UHFRC	34.24	1.51	11.18	1.23
6THFRC	32.05	1.55	14.52	1.60
CNCC1	16.45	1.93	7.75	0.49
CNCC2	17.60	1.91	7.31	0.47
CNCC3	18.89	1.85	7.08	0.44
6THFR-CNCC1	28.07	1.62	20.16	2.21
6THFR-CNCC2	29.37	1.60	19.18	2.14
6THFR-CNCC3	30.22	1.57	18.33	2.04

3 RESULTS AND DISCUSSION

3.1 Quantitative X-Ray Diffraction Analysis (QXDA) of Nano-Matrix

Table 2 shows the quantitative analysis with Rietveld refinement of cement paste and nanocomposites containing 1, 2 and 3 wt% CNC. As can be seen from Table 2, CNC1 nanocomposite reduced the amount of $Ca(OH)_2$ by about 28% reduction. This indicates that an obvious consumption of $Ca(OH)_2$ crystals mainly due to the effect of pozzolanic reaction in the presence of CNC and good dispersion of CNC in the matrix leads to produce more amorphous C-S-H gel [Wei et al. 2012, Hakamy et al. 2014a]. On the other hand, For CNC3nanocomposites, the amount of $Ca(OH)_2$ was decreased by about 16% reduction compared to cement paste. This may be attributed to agglomerations of CNC at high contents which lead to relatively poor dispersion of CNC and hence relatively poor pozzolanic reaction.

3.2 Porosity and density

The porosity and density of cement paste, un-treated hemp fabric-reinforced cement composites (UHFRC), 6THFRC composites, nanocomposites and treated hemp fabric-reinforced calcined nanoclay-cement nanocomposites (6THFR-CNCC) are shown in Table 3. It can be seen that the addition of CNC decreases the porosity and increases density of nanocomposites and 6THFR-CNCC nanocomposites when compared to control cement paste and 6THFRC composites. For 6THFR-CNCC1 nanocomposite, the porosity decreased by 12.4% and the density increased by 4.5% compared to 6THFRC composites. This indicates that CNC has filling effect in the porosity of cement paste composites with and without 6 treated hemp fabric, in which nanocomposite matrix become more consolidated microstructure [Jo et al. 2007].

3.3 Flexural strength

Flexural strength of cement paste, un-treated hemp fabric-reinforced cement composite (UHFRC), 6THFRC composites, nanocomposites (CNC) and treated hemp fabric reinforced-nanocomposites (6THFR-CNCC) are shown in Table 3. The optimum Hemp fabric content was found to be 6.9 wt%, in which the flexural strength is increased from 5.42 to 12.64 MPa, about 133.2% increase compared to cement paste. In addition, Table 3 also shows the effect of the NaOH treatment of Hemp fabric on the flexural strength of 6THFRC composites. It can be clearly seen that the flexural strength of 6THFRC composites is increased from 12.64 to 14.52 MPa, about 14.9% increase compared to 6UHFRC composite.

Overall, the incorporation of CNC into the 6UHFRC composite led to significant enhancement in the flexural strength of all treated Hemp fabric reinforced nanocomposites. The flexural strength of 6THFR-CNCC1 is increased from 14.52 to 20.16 MPa, about 38.8% increase compared to 6UHFRC composite. This improvement clearly indicates the effectiveness of CNC in consuming calcium hydroxide (CH), supporting pozzolanic reaction and filling the micro pores in the matrix [Wei et al. 2014]. Thus the microstructure of nanocomposite matrix is denser than the cement matrix [Shebl et al. 2009]. Consequently, the treated hemp fabric-nanocomposite matrix interfacial bonding is mostly improved, especially in the case of using 1wt% CNC, which is evident from the higher flexural strength value. Moreover, the addition of more CNC (i.e. 2 wt %) led to a significant reduction in flexural strength due to an increase in porosity. Nevertheless the addition of CNC improved the flexural strength of treated hemp fabric reinforced cement composites. For example, in this study, although the flexural strength of composite with 3 wt% CNC decreased compared to composite with 1wt% CNC but it is still higher than the 6UHFRC composite.

3.4 Fracture Toughness

Fracture toughness of cement paste, un-treated hemp fabric-reinforced cement composite (UHFRC), 6THFRC composites, nanocomposites and 6THFR-CNCC nanocomposites are shown in Table 3. It can be seen that the fracture toughness of 6THFR-CNCC1 nanocomposite increased by 38.1% compared to 6THFRC composite. This is attributed to the fact that the CNC modified the matrix through pozzolanic reaction and reduced the $Ca(OH)_2$ content. Thus, good interfacial bond between the nanomatrix and the treated hemp fibres was achieved [Hakamy et al. 2014, Alamri et al. 2012]. However, facture toughness of 6THFR-CNCC nanocomposites gradually decreases, when CNC content increases after the optimum content of 1 wt%. This is attributed to the poor dispersion of high content of CNC into the matrix, which leads to increase in porosity and weaken the interfacial bond between the fibres and the matrix.

Fig. 3 (a-b) shows the SEM micrographs of the fracture surface and fibre-matrix interface of 6THFR-CNCC1 and 6THFR-CNCC3 nanocomposite. A variety of mechanisms such as fibre-matrix interface, fibre pull-out and rupture fibre are observed. The examination of fracture surface of 6THFR-CNCC1 nanocomposite show very good fibre-matrix interfacial bonding in terms of ruptured fibres (Fig. 3a). However, in 6THFR-CNCC3 nanocomposite (Fig. 3b), debonding of fibre was observed which indicated relatively poor adhesion between the fibre and the matrix.

4 SUMMARY

The paper presents the influence of calcined nanoclay (CNC) on microstructures and mechanical properties of treated hemp fabric-reinforced cement nanocomposite. The optimum content of hemp fabric is found to be 6.9 wt% (6 hemp fabric layers) and the optimum content of CNC was found to be 1 wt%. The 6THFR-CNCC1 nanocomposites increased the flexural strength (14.9%) and the fracture toughness (38.1%) compared to the 6THFRC composites. The QXDA analysis also showed that the addition of 1 wt% CNC in cement paste reduced the amount of $Ca(OH)_2$ and increased the amount of C-S-H gel. However, the addition of more CNC (beyond optimum content- 1 wt %) into the treated hemp fabric-reinforced composites adversely affected the porosity and fracture toughness.

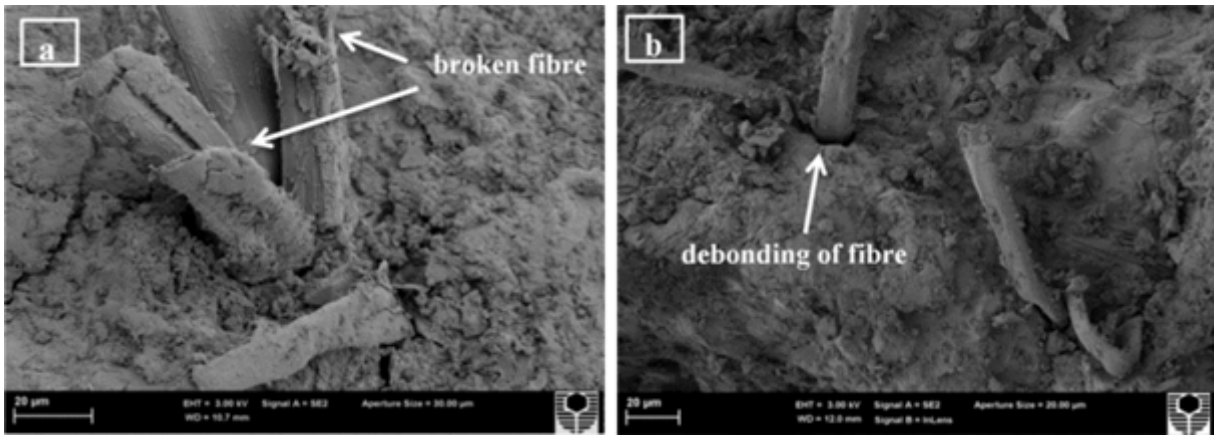

Fig. 3. SEM images of the fracture surfaces for (a) 6THFR-CNCC1 and (b) 6THFR-CNCC3 nanocomposites

5 REFERENCES

Alamri, H.; Low, I.M.; Microstructural, mechanical, and thermal characteristics of recycled cellulose fiber-Halloysite-epoxy hybrid composites. Polym Compos, Feb 2012, 33, 589-600.

Hakamy, A.; Shaikh, F.U.A.; Low, I.M.; Characteristics of hemp fabric reinforced nanoclay–cement nanocomposites. Cem Concr Compos. Jul 2014, 50, 27–35.

Jo, B.; Kim C.; Tae G.; Park J.; Characteristics of cement mortar with nano-SiO_2 particles. Constr Build Mater. Jun 2007, 21(6), 1351–1355.

Nazari, A.; Riahi, S.; The effects of Zinc Oxide nanoparticles on flexural strength of self-compacting concrete. Compos Part B. Mar 2011, 42(2),167–175.

Pacheco, F.; Jalali, S.; Cementitious building materials reinforced with vegetable fibres: a review. Constr Build Mater. Feb 2011, 25 (2), 575-581.

Sanchez, F.; Sobolev, K.; Nanotechnology in concrete - A review. Constr Build Mater. Nov 2010, 24 (11), 2060–2071.

Sedan, D.; Pagnoux, C.; Smith, A.; Chotard, T.; Mechanical properties of hemp fibre reinforced cement: influence of the fibre/matrix interaction. J Eur Ceram Soc. 2008, 28 (1), 183-192.

Shebl S.; Allie L.; Morsy M.; Aglan H.; Mechanical behavior of activated nano silicate filled cement binders. J Mater Sci. 2009, 44, 1600-1606.

Wei J.; Meyer C.; Sisal fiber-reinforced cement composite with Portland cement substitution by a combination of metakaolin and nanoclay. J Mater Sci. 2014, 49, 7604–7619.

Wei, Y.; Yao, W.; Xing, X.; Wu, M.; Quantitative evaluation of hydrated cement modified by silica fume using QXRD, 27Al MAS NMR, TG–DSC and selective dissolution techniques. Constr Build Mater. Nov 2012, 36, 925–932.